Dependence of samarium-soil interaction on samarium concentration: implications for environmental risk assessment

Oriol Ramírez-Guinart, Aitor Salaberria, Miquel Vidal and Anna Rigol*

Department of Chemical Engineering and Analytical Chemistry, Faculty of Chemistry, University of Barcelona, Martí i Franqués 1-11, 08028, Barcelona, Spain.

*Corresponding author: telephone, (+34) 93 403 9274; fax, (+34) 93 402 1233; e-mail, *annarigol@ub.edu*

ABSTRACT

The sorption and desorption behaviour of samarium (Sm), an emerging contaminant, was examined in soil samples at varying Sm concentrations. The obtained sorption and desorption parameters revealed that soil possessed a high Sm retention capacity (sorption was higher than 99% and desorption lower than 2%) at low Sm concentrations, whereas at high Sm concentrations, the sorption-desorption behaviour varied among the soil samples tested. The fractionation of the Sm sorbed in soils, obtained by sequential extractions, allowed to suggest the soil properties (pH and organic matter solubility) and phases (organic matter, carbonates and clay minerals) governing the Sm-soil interaction. The sorption models constructed in the present work along with the sorption behaviour of Sm explained in terms of soil main characteristics will allow properly assessing the Sm-soil interaction depending on the contamination scenario under study. Moreover, the sorption and desorption K_d values of radiosamarium in soils were strongly correlated with those of stable Sm at low concentrations ($r = 0.98$); indicating that the mobility of Sm radioisotopes and, thus, the risk of radioactive Sm contamination can be predicted using data from low concentrations of stable Sm.

Keywords: rare earth element, soil contamination, sorption isotherm, solid-liquid distribution coefficient, desorption.

Capsule: Soil phases involved in Sm interaction vary depending on Sm concentration and this fact should be considered for a proper risk assessment of a soil contaminated with Sm or other lanthanides.

1. Introduction

Rare earth elements (REEs), especially lanthanides, have become important in agriculture and industrial activities because of their unique physicochemical properties (Awual et al., 2013). Increased anthropogenic inputs of REE in the environment through mining (Jinxia et al., 2010; Li et al., 2013; Liang et al., 2014), the discharge of industrial effluents (Ali, 2014; He et al., 2010) and the extensive application of REE-enriched fertilisers (Cao et al., 2001; Pang et al., 2001; Tyler, 2004; Zhang et al., 2000) have led to the contamination of watersheds and soil.

Trivalent lanthanide samarium (Sm) is a REE emerging contaminant that has been found in wastes resulting from agricultural and industrial activities (He et al., 2010; Pang et al., 2001). There are many evidences of watersheds that, due to contamination by industrial wastes, specially mine tailings, contain Sm at concentration levels several orders of magnitude higher than the water background value in Chinese rivers (around 10^{-4} μg L^{-1}, that is, ≈ 10^{-9} meq L^{-1}) (Meng and Li, 2008), such as the case of Baotou Area containing up to 130 μg Sm L^{-1} (2.4×10^{-3} meq L^{-1}) (Lu et al., 1995). Besides, some works have also reported that the Sm concentration in lands treated with REE-rich fertilisers or irrigated by the abovementioned contaminated liquid sources is abnormally higher, e.g., 25 mg kg^{-1} in Jiangxi area, China (Zhu et al., 2002) or 492 mg kg^{-1} in Bayan Obo, China (Jinxia et al., 2010), compared to the soil background value in China (5 mg kg^{-1}) (Wei et al., 1991) and the world average (1 mg kg^{-1}) (Wang et al., 1989). This concomitant soil contamination is also of special concern since soils can act as sink of Sm that can be further incorporated in the food chain or reintroduced into

water sources due to irrigation and raining processes (Liang et al., 2005). Consequently, there is increasing concern about the potential harmful effects of trivalent REE contamination on non-human biota and humans (Ali, 2014; Humsa and Srivastava, 2015; Jinxia et al., 2010; Li et al., 2013; Zhao et al., 2017; Zhu et al., 1997). Although trivalent REE present limited toxicity for humans, human exposure to high dose of these compounds can cause adverse effects such as pneumonitis, whereas long-term exposure can cause more harmful effects such as pneumoconiosis (Hirano and Suzuki, 1996) or abnormal neurobehavioral development (Feng et al., 2005).

Furthermore, Sm radioisotopes are present in spent nuclear fuel and radioactive wastes (GRS, 2012), as the beta-emitting ^{151}Sm radioisotope with a relatively long half-life ($T_{1/2}$ = 90 years), thus being an element of concern in the mid-term (100-500 years) management of low- and intermediate-level radioactive wastes (Rego et al., 2011).

The interaction of trivalent lanthanides (Ln(III)) with geological media is mediated by the formation of surface complexes with clay minerals, metal oxides and organic matter (OM) solid particles, which depend on factors affecting Ln(III) aqueous speciation and sorption site availability, such as pH, organic matter solubility and mineralogy (Fan et al., 2010; McCarthy et al., 1998; Ramírez-Guinart et al., 2017; Takahashi et al., 1998; Ye et al., 2014). Ln(III) sorption by solid mineral particles increases with increasing pH due to the increasingly negative net surface charge and the predominating Ln^{3+} and cationic hydroxyl complexes (Fan et al., 2010; Geckeis and Rabung, 2008; Wenming et al., 2001). Although some studies have indicated a high affinity of Ln(III) for OM particles (Pang et al., 2001; Pourret and Martinez, 2009; Shan et al., 2002) and carbonate minerals like calcite or aragonite (Sutton, 2009), the presence of large amounts of dissolved humate compounds or carbonates may decrease Ln(III) sorption as Ln(III) can form soluble anionic humate and carbonate complexes (Dupré et al., 1999; Shan et al., 2002; Wenming et al., 2001; Xiangke et al., 2000;

Zhong and Mucci, 1995). Moreover, the mobility of Ln(III) in a terrestrial ecosystem depends on its concentration (Galunin et al., 2009, 2010) and soil properties (Jones, 1997; Zhu et al., 1993).

There are few studies examining the effect of geochemical factors on the interaction of REEs with soil and sediments (Cao et al., 2000, 2001; Li et al., 2000, 2001; Ramírez-Guinart et al., 2017; Shan et al., 2002; Wang et al., 2011). To the best of our knowledge, none have simultaneously evaluated the effect of soil properties and REE concentration on their sorption-desorption behaviour. The objective of this study is to examine the interaction between Sm and soil samples with contrasting edaphic properties as a function of Sm concentration, assessing five types of soils to account for different contamination scenarios. The dependency of Sm sorption and desorption parameters on Sm concentration was examined by constructing Sm sorption isotherms, while the soil phases and mechanisms involved in Sm sorption were assessed by a sequential extraction procedure. Finally, the sorption and desorption parameters here obtained for low concentrations of stable Sm were compared with those gathered for Sm radioisotopes in a previous work from the same soils tested here (Ramírez-Guinart et al., 2017).

2. Materials and Methods

2.1. Soil samples

For the present study five soil samples presenting contrasting properties (see Table 1) were selected from a collection of soils for which the interaction of Sm radioisotopes was extensively studied in a previous work (Ramírez-Guinart et al., 2017). All samples were taken from the surface layer (0-10 cm), air-dried, sieved though a 2-mm mesh, homogenised with a roller table and stored in plastic bottles until analysis. The following physical-chemical characterisation was performed. Particle size distribution (clay, silt and sand percentages) was determined by the pipette method (Burt, 2004), except for DUBLIN soil, were the clay

101 percentage was determined by X-ray diffraction, due to the high organic matter content of this
102 soil. The carbonate ($CaCO_3$) content was determined by using the calcimeter Bernard method
103 (Muller and Gastner, 1971). The loss on ignition (LOI) content was determined as the loss of
104 soil weight by ashing 2 g of each soil sample (previously oven-dried overnight at 110ºC) at
105 450°C for 16 h in a muffle furnace. The cation exchange capacity (CEC) was determined as
106 the sum of exchangeable bases plus the exchangeable acidity obtained by displacement with
107 $BaCl_2$-triethanolamine solution buffered at pH 8.2 (Burt, 2004) and the specific surface area
108 of soils (SSA) was determined by N_2 adsorption after degasification at 100ºC (Fagerlund,
109 1973). In addition, the solutions obtained after equilibrating the soil samples with deionised
110 water under the same conditions as those of the sorption tests (see Section 2.2.) were also
111 characterised in terms of pH, dissolved organic carbon (DOC) and dissolved inorganic carbon
112 (DIC), and concentration of major cations (Ca, Mg, K and Na). The DOC content was
113 measured using a Total Organic Carbon analyser (Shimadzu TOC-5000 A) (Shimadzu, Japan)
114 with a previous acidification with HCl to a pH of 3 to remove the carbonates in solution. The
115 DIC content was calculated as the difference between the total carbon content, determined as
116 the DOC but without the acidification step, and the DOC content. The concentration of major
117 cations was determined by inductively coupled plasma optical emission spectrometry (ICP-
118 OES) (Thermo-Jarrell Ash 25 and Perkin Elmer Optima 3200 RL, USA). Details about the
119 methodologies used for the physical-chemical characterisation of soil samples are described
120 in Ramírez-Guinart et al. (2016).
121 Most of the soil properties (see Table 1) varied within wide ranges, thus being representative
122 of different environmental scenarios. CABRIL and ASCO are mineral soils with low amounts
123 of organic matter (OM), the latter one being a calcareous soil with high carbonate content and
124 a basic pH. ANDCOR and DUBLIN are organic soils with an acidic pH and high amounts of
125 soluble organic matter, here represented with dissolved organic carbon content (DOC).
126 Finally, DELTA2 has a basic pH and significant organic matter content, but moderate

amounts of soluble organic matter. It had the highest contents of carbonate and clay (fraction of particles with size < 0.002 mm) among all the soil samples tested.

2.2. Sorption and desorption experiments

Batch sorption experiments were carried out with each soil sample to quantify K_d (Sm) values at varying initial Sm concentrations. The sorption test consisted of mixing 2 g of soil sample with 45 mL of double-deionised water in 80-mL polypropylene centrifuge tubes and shaking the suspensions for 16 hours using an end-over-end shaker at 60 rpm. Afterwards, each resulting suspension was spiked with 5 ml of a solution containing a known amount of stable Sm, prepared from 99.9%-pure $Sm(NO_3)_3$ (Sigma-Aldrich, Germany), to give an initial Sm concentration (C_i) of between 0.01 and 10 meq L^{-1} (a minimum of 9 different concentrations were tested). Before each series of sorption experiments, aliquots from the Sm stock solutions prepared to spike the batch sorption assays were analysed to determine the initial Sm concentration. Sorption of Sm in the laboratory ware used for the batch sorption and desorption assays was considered negligible, as it was demonstrated in a previous work (Ramírez-Guinart et al., 2016) for the case of Am, a chemical analogue of Sm. The selected Sm concentrations allow to cover different contamination scenarios, i.e., from soil affected by slightly contaminated liquid sources, such as watersheds or groundwater located far away from the contamination source point, to those soils affected by high Sm concentration sources, such as REE mine tailings. The suspensions were equilibrated again for 24 hours and centrifuged (12,880 *g* for 30 minutes at 10ºC) using a Beckman J2-HS centrifuge with a JA-14 rotor (Beckman, Ireland). The supernatants were decanted, filtered through 0.45-µm nylon syringe filters and transferred to 20-mL polyethylene vials before pH analysis. Blank sorption assays were carried out in parallel following the procedure above, but adding 5 mL of double-deionised water instead of Sm solution. The supernatants obtained from sorption and blank

151 assays were diluted with 1% HNO_3 and stored at 4ºC until analysis. Aliquots of the blank
152 sorption supernatants were used to determine relevant soil parameters as explained in 2.1.

153 The reversibility of Sm sorption into soil was evaluated by applying a desorption test to the
154 40°C-dried soil residues obtained from the previous sorption experiments carried out at
155 selected initial Sm concentrations (C_i approximately 0.01, 0.1, 3 and 9 meq L^{-1}). Soil residues
156 were dried before the desorption step to simulate the ageing process that occurs in field
157 scenarios. A single extraction was performed under the same experimental conditions as the
158 sorption test, using double-deionised water as the contact solution. The obtained supernatants
159 were centrifuged, decanted, filtered through 0.45-µm nylon syringe filters and transferred to
160 20-mL polyethylene vials. The collected supernatants were then diluted with 1% HNO_3 and
161 stored at 4ºC until analysis.

162 The sorption and desorption K_d data obtained for low concentrations of stable Sm were
163 compared with those gathered for Sm radioisotopes in a previous work from the same soils
164 tested here (Ramírez-Guinart et al., 2017).

165

166 *2.3. Sequential extraction procedure*

167 Sequential extractions were applied to the soils contaminated with stable Sm obtained from
168 the previous sorption experiments to achieve the following sorbed Sm fractions: (F1) 0.01
169 mol L^{-1} $CaCl_2$, electrostatically weakly bound (such as exchangeable elements) (Houba et al.,
170 2000); (F2) 0.43 mol L^{-1} CH_3COOH, sensitive to acidification processes (e.g., bound to
171 carbonates) (Quevauviller et al., 1997); (F3) 0.1 mol L^{-1} NaOH, bound to organic matter,
172 mainly organic acids (e.g., humic and fulvic acids) (Shand et al., 1994); and (F4) residue,
173 bound to non-soluble organic matter and/or to soil mineral phases (e.g., humin or clay
174 minerals).

175 Two soil residues from sorption tests corresponding to a low and a high Sm concentration (*Ci*
176 approximately 0.06 and 6 meq L^{-1}, respectively) were selected for each soil sample. The
177 extractions were performed by mixing 1 g of soil residue with 40 mL of extractant solution
178 and shaking the mixture in an end-over-end shaker for 24 hours at room temperature.
179 Afterwards, the soil suspensions were centrifuged and the supernatants decanted, filtered
180 through 0.45-µm nylon syringe filters, transferred to plastic vials, diluted with 1% HNO_3 and
181 stored at 4ºC until analysis.

182 *2.4. Analytical measurements*

183 Sm concentration in the filtered solutions from the different tests was determined by
184 inductively coupled plasma optical emission spectroscopy (ICP-OES) at a wavelength of
185 359.3 nm, using Thermo Jarrell Ash 25 and PerkinElmer Optima 3200 RL (PerkinElmer,
186 USA). For Sm concentrations lower than the ICP-OES quantification limit (30 µg L^{-1}), Sm
187 concentrations were obtained from measurements of the ^{147}Sm isotope by inductively coupled
188 plasma mass spectrometry (ICP-MS), using Perkin-Elmer Elan-6000 (PerkinElmer, USA).
189 The Sm quantification limit for ICP-MS was 10 ng L^{-1}.

190 *2.5. Calculation of sorption and desorption parameters*

191 The Sm solid-liquid distribution coefficients of the sorption process, K_d (Sm), corresponding
192 to the ratio of the Sm concentration sorbed into the soil (C_{sorb}, meq kg^{-1}) to the Sm
193 concentration remaining in the liquid phase after the sorption process (C_{eq}, meq L^{-1}), were
194 calculated as follows:

$$K_d\,(L\,kg^{-1}) = \frac{C_{sorb}}{C_{eq}} = \frac{(C_i - C_{eq})\frac{V}{m}}{C_{eq}} \qquad [1]$$

where V is the liquid phase volume (L), m the soil sample dry weight (kg), and C_i the initial Sm concentration (meq L^{-1}). In addition, sorption percentages (S, %) were calculated as follows:

$$S\,(\%) = \frac{(C_i - C_{eq})}{C_i} \times 100 \quad [2]$$

The solid-liquid distribution coefficients of the desorption process, that is, the ratio of the Sm concentration in the soil ($C_{sorb,des}$, meq kg^{-1}) to that in the liquid phase after the desorption process ($C_{eq,des}$, meq L^{-1}), were calculated with the following equation:

$$K_{d,des}\,(L\,kg^{-1}) = \frac{C_{sorb,des}}{C_{eq,des}} = \frac{C_{i,des} - C_{eq,des} \times \frac{V}{m}}{C_{eq,des}} \quad [3]$$

$C_{i,des}$, in meq kg^{-1}, is C_{sorb} corrected by the amount of Sm present in the small volume (few millilitres) of solution remaining after the sorption experiment (V_{res}), which is incorporated into the solid phase after drying:

$$C_{i,des} = C_{sorb} + C_{eq} \times \frac{V_{res}}{m} \quad [4]$$

Desorption percentages (D, %) were calculated as follows:

$$D\,(\%) = \frac{C_{eq,des} \times V}{C_{i,des} \times m} \times 100 \quad [5]$$

2.6. Construction and fitting of sorption isotherms

Sorption isotherms were constructed by plotting C_{sorb} vs. C_{eq} and K_d vs. C_{sorb} obtained with the different Sm concentrations assayed. Moreover, C_{sorb} vs. C_{eq} isotherms were fitted with Freundlich, Langmuir and linear sorption models. The sorption models are described in Hinz (2001).

The Freundlich isotherm equation is defined as follows:

$$C_{sorb} = K_f \times C_{eq}^{N} \quad [6]$$

where C_{sorb} (meq kg^{-1}) is the sorbed concentration of the contaminant, C_{eq} (meq L^{-1}) the contaminant concentration in solution after the sorption process, K_f (meq$^{(1-N)}$ L^N kg^{-1}) the Freundlich constant describing the partitioning of the contaminant between the solid and liquid phases at a given initial concentration, and N (dimensionless) the site heterogeneity.

The Langmuir isotherm equation is defined as follows:

$$C_{sorb} = \frac{b \times K \times C_{eq}}{1 + K \times C_{eq}} \quad [7]$$

where b (meq kg^{-1}) and K (L meq^{-1}) estimate the maximum sorption capacity of the soil and the bonding energy of the sites, respectively.

When the contaminant partitioning is constant over the whole concentration range, a linear isotherm can be defined as follows:

$$C_{sorb} = K_{d,\,linear} \times C_{eq} \quad [8]$$

For both Freundlich and Langmuir isotherms, $K_{d,linear}$ can also be deduced from the slope of the C_{sorb} vs C_{eq} correlation at the low concentration range.

Curve Fitting Toolbox™ (cftool), included in the Matlab R2009a software (MathWorks Inc., 2009) to fit curves to one-dimensional data, was used to fit the sorption isotherms to the abovementioned sorption models. The fitting coefficients were constrained as positive values, with confidence limits ≥95%, applying non-linear least squares with the trust-region algorithm option.

3. Results and Discussion

3.1. Description of Sm sorption isotherms

Figure 1 shows the Sm sorption isotherms (C_{sorb} vs. C_{eq} and K_d vs. C_{sorb}) for the five soil samples analysed. For all soils, the sorption data (C_{sorb} and C_{eq}) were satisfactorily distributed

231 in the entire range of concentrations evaluated, which made possible to analyse the effect of
232 Sm concentration on the soil capacity to sorb Sm as well as to properly fit the data to sorption
233 models. Nearly linear-shaped C_{sorb} vs. C_{eq} isotherms were obtained for DELTA2 and
234 DUBLIN soil samples, showing constant Sm sorption capacity irrespective of the initial Sm
235 concentration and, thus, indicating no saturation of sorption sites. However, K_d (Sm) values
236 appeared to be slightly lower at low Sm concentrations, suggesting that Sm sorption in the
237 solid phase might be affected by competing processes that keep this element in solution. Thus,
238 the formation of soluble chelates with dissolved organic matter has been demonstrated to play
239 a key role in the interaction of trivalent lanthanides and actinides elements in mineral phases
240 (Ramírez-Guinart et al., 2017; Ye et al., 2014). Besides, in the low concentration range of the
241 sorption isotherms, the sorption of cationic species present in solution may also decrease the
242 sorption of Sm in the solid phase (Pathak and Choppin, 2007).

243 Regarding ANDCOR, ASCO and CABRIL, the curve-shaped C_{sorb} vs. C_{eq} isotherms indicated
244 that Sm sorption was strongly influenced by Sm concentration. For these soils, the slope of
245 the C_{sorb} vs. C_{eq} isotherms decreased with increasing Sm concentration and a pseudo-plateau
246 was reached at high Sm concentrations, indicating either a saturation of the Sm sorption sites,
247 or the presence of sorption sites with contrasting affinities for Sm, that is, non-specific
248 sorption sites and high affinity sites such as silanol groups in clay minerals, carboxylic groups
249 in organic matter or specific carbonate-like minerals (Ramírez-Guinart et al., 2017; Shanbhag
250 and Morse, 1981; Takahashi et al., 1998).

251 Examination of the K_d vs. C_{sorb} isotherms, as suggested by Hinz (2001), revealed a relatively
252 constant partitioning at the lowest Sm concentration range ($C_i < 0.6$ meq L^{-1}, corresponding to
253 $C_{sorb} < 20$ meq kg^{-1}) for ANDCOR and CABRIL, followed by a linear decrease in K_d (Sm)
254 values at higher Sm concentrations. These sorption patterns are associated with Langmuir-

type sorption behaviour as they indicate the existence of sorption sites with similar affinity for Sm that become saturated at increasing Sm concentrations. Conversely, the K_d vs. C_{sorb} isotherm of ASCO showed a sharp decrease in Sm sorption at low concentrations followed by constant K_d values at $C_i > 0.6$ meq L^{-1}. This sorption pattern indicates that Sm was sorbed onto sites with a much higher affinity at low Sm concentrations than at higher Sm concentrations, which can be linked to Freundlich-type sorption behaviour.

3.2. Analysis of the Sm-soil interaction at varying Sm concentrations

Table 2 summarises the sorption and desorption parameters gathered from the five soil samples at four Sm concentrations. At the lowest Sm concentration, all soils showed high Sm sorption capacity, with K_d (Sm) values always $>10^3$ L kg^{-1} and sorption percentages (S) close to 100%. At this Sm concentration, the Sm remaining in solution after the sorption process (C_{eq}) did not exceed the maximum Sm concentration permitted in drinking water (4.8 10^{-4} meq L^{-1}) proposed by Moikin (1993).

At higher sorbed Sm concentrations, K_d (Sm) remained almost constant for DELTA2 and DUBLIN. However, for ANDCOR, CABRIL and ASCO, K_d (Sm) values dropped several orders of magnitude and sorption percentages plummeted to around 50% at the highest Sm concentration, indicating that Sm sorption occurs at low-affinity sites at these high concentrations. Therefore, for this type of soil, a single value of K_d (Sm) cannot be used for risk assessment, but instead a concentration-dependent best estimate should be used according to the type of contamination.

With respect to the desorption parameters, $K_{d,des}$ values were always $>10^3$ L kg^{-1} and the desorption percentages (D %) extremely low (< 2%), suggesting that most of the Sm incorporated into these soils was irreversibly sorbed regardless of the soil properties or the amount of Sm previously sorbed into the soil. In addition, the $K_{d,des}/K_d$ ratio was constant and

close to 1 at all the Sm concentrations tested for DELTA2 and DUBLIN. For ANDCOR, CABRIL and ASCO, the $K_{d,des}/K_d$ ratio increased by up to tens to hundreds at increasing Sm concentrations. These sorption-desorption patterns suggest that $K_{d,des}$ values are similar for all the soil samples after the drying process and become less dependent on the initial Sm concentration. However, despite the high irreversibility of Sm sorption into soil, for the highest levels of soil contamination, the Sm concentration in solution after the desorption process ($C_{eq,des}$) exceeded the maximum Sm concentration permitted in drinking water (4.8×10^{-4} meq L^{-1}).

3.3. Proposal of Sm sorption parameter values for different environmental contamination scenarios

As it has been shown, the Sm sorption into soil is heavily influenced by its concentration and soil properties and thus, different Sm sorption data should be used to assess properly the Sm-soil interaction depending on the contamination scenario under study. To this end, the sorption data gathered at the lowest Sm concentration range were fitted to a linear model and the derived K_d values ($K_{d,linear}$ (Sm) values) are considered to be appropriate best estimates of K_d (Sm) to assess risk of soil contamination for low Sm concentrations. Whereas, the entire sorption isotherms were fitted to Freundlich and Langmuir sorption models so as to describe the Sm-soil interaction expected in those contamination events involving high Sm concentrations. Table 3 summarises the parameters derived from the best fitting of the sorption isotherms constructed for the soils tested. The graphical representation of the best fitting of the sorption isotherms for the whole range of concentrations can be found in Figure S1 in Supplementary Information.

As anticipated, the sorption isotherms of DELTA2 and DUBLIN were perfectly described by a Freundlich model, with N values close to 1. Therefore, there was no saturation of the sorption sites and all the sites presented similar affinity for Sm (pseudo-linear sorption

behaviour). However, the N value slightly higher than 1, especially in the case of DUBLIN, suggests that Sm sorption was slightly decreased at low Sm concentrations. Considering the high content of dissolved organic matter in these soils, such Sm sorption behaviour at low Sm concentrations might result from the formation of stable and soluble negatively-charged Sm-humate complexes. The Freundlich model was also the most appropriate for describing the Sm sorption isotherm of ASCO. The N value (much lower than 1) indicated Sm sorption at sites with varying affinity for Sm, suggesting that the decrease in the capacity of ASCO to sorb Sm at high Sm concentrations was due to saturation of the available high-affinity sites, as deduced from K_d vs. C_{sorb}.

The Langmuir model best described the Sm sorption behaviour of ANDCOR and CABRIL. These soil types presented a limited number of sorption sites (parameter *b* of the Langmuir model around 120-130 meq Sm per kg) with a relatively constant and low affinity for Sm. The Sm sorption sites available in ANDCOR seem to have a much lower bonding energy than those of the other soil samples.

Soil contaminated by radioactive liquid waste is expected to contain a much smaller concentration of Sm than that contaminated by stable Sm isotopes. Thus, the $K_{d,linear}$ (Sm) derived at the lowest concentration range (C_i = 0.01 – 0.2 meq L^{-1}) (Table 3) and the $K_{d,des}$ (Sm) data obtained at the lowest Sm concentration assayed (Table 2) were compared with the sorption-desorption K_d data obtained for ^{151}Sm in a previous study ($C_i = 10^{-5}$ meq L^{-1}) (Ramírez-Guinart et al., 2017) with the aim of proving that K_d data of low concentrations of stable Sm can be used to foresee the soil interaction of Sm radionuclides. As can be ascertained from Figure 2, the two sets of data were highly correlated (r = 0.98) and the paired tests revealed no significant differences between the two sets of data ($p > 0.05$). This demonstrated that the sorption capacity of soil was similar for Sm radioisotopes and low

concentrations of stable Sm, thus suggesting that the data obtained with low Sm concentrations can also be used for assessing the risk of contamination with Sm radioisotopes.

3.4. Soil characteristics associated with Sm sorption as a function of Sm concentration

The contrasting sorption behaviour observed among the soil types led us to evaluate the relationship between the concentration-dependent capacity of soil to sorb Sm and the sorption mechanisms responsible for this soil-Sm interaction by gaining knowledge about the fractionation of the Sm sorbed in soils at different Sm concentrations. Figure 3 shows the Sm fractionations obtained with the sequential extraction procedure applied to the soil residues from the sorption experiments performed at low and high Sm concentrations (0.06 and 6 meq L^{-1}, respectively). The sequential extraction approach indicates the soil phases involved with Sm interaction and is an excellent tool for comparing the level of contamination of the soil types at different Sm concentrations.

Almost 100% of the Sm sorbed into DELTA2 at low and high Sm concentrations remained in the residual fraction, showing that this soil has a large number of high-affinity sorption sites for Sm. As DELTA2 displays a basic pH as well as high contents of clay and OM, the high and linear Sm sorption (K_d always > 10^4 L kg^{-1}) previously observed can be attributed to Sm forming complexes with high-affinity sites such as hydroxyl groups in clay minerals or carboxylic and phenolic groups in the insoluble OM (humin) fraction (Pourret et al., 2009; Ye et al., 2014). Moreover, due to the moderate amount of dissolved organic compounds, only a small fraction of Sm will form complexes with dissolved organic compounds (soluble Sm-humate complexes) that are weakly sorbed due to Coulomb repulsion with soil surfaces (Shan et al., 2002; Takahashi et al., 1998). As with DELTA2, the amount of Sm sorbed into DUBLIN at a low Sm concentration was similar to that at a high Sm concentration. However, only around 40% of Sm remained in the residual fraction, the majority occurring in the non-residual fraction corresponding to soluble OM at an alkaline pH. Based on the properties of

353 DUBLIN (extremely high loss on ignition and negligible clay content), this Sm fractionation
354 points to a sorption mainly mediated by complexation with more labile (humic and fulvic
355 acids) or insoluble (humin) OM fractions, rather than with clay minerals. The lower residual
356 fraction of Sm in DUBLIN agrees with its considerably lower K_d (Sm) when compared to that
357 of DELTA2. Although a high OM content seems to provide enough high-affinity sorption
358 sites to ensure linear sorption across the entire Sm concentration range tested, Sm sorption in
359 DUBLIN ($K_{d,linear}$ = 2,400 L kg^{-1}) was lower than that in DELTA2 ($K_{d,linear}$ = 17,000 L kg^{-1}).
360 This difference can be explained by the high content of dissolved organic compounds in
361 DUBLIN (290 mg kg^{-1}) resulting from the different nature of the OM present in DUBLIN and
362 its acid pH, suggesting that the negatively-charged Sm-humate complexes generated remain
363 in solution due to electrostatic repulsion with soil surfaces (Xiangke et al., 2000; Ye et al.,
364 2014).

365 The Sm fractionation patterns for the remaining soil samples varied according to the Sm
366 concentration, showing increased Sm sorption into F2 (sensitive to acidification) and/or F1
367 (exchangeable) fractions at high Sm concentrations. These results indicate that significant
368 amounts of Sm were sorbed at low-affinity sorption sites, which is consistent with the
369 concentration dependency of Sm sorption (i.e., significantly decreased sorption capacity at
370 high Sm concentrations) shown by the sorption isotherms of these soils (Figure 1). Among
371 these, ANDCOR presented the lowest Sm sorption capacity despite having moderate amounts
372 of clay and OM (18% and 19%, respectively). A reason is that its acid pH restricts the number
373 of sorption sites available (low net negative surface charge due to low deprotonation of
374 organic functional groups) and that a significant amount of Sm is slightly reactive with the
375 soil surface due to the formation of highly soluble Sm-humate species (dissolved organic
376 content = 78 mg kg^{-1}) (Ho Lee et al., 2011; Jin et al., 2014; Ye et al., 2014). By contrast, the
377 relatively moderate Sm sorption capacity of CABRIL can be attributed to an insufficient
378 number of high-affinity sorption sites resulting from its low content of OM and, on the other,

379 from its neutral pH, which limits the pool of sorption sites from clay minerals available to
380 interact with the cationic Sm species.

381 ASCO exhibited the highest Sm sorption capacity at low Sm concentrations and the lowest at
382 high Sm concentrations, thus denoting the presence of a very limited number of extremely
383 high-affinity sites. The same amounts of Sm were observed in the residual and F2 fractions at
384 low Sm concentrations, whereas Sm was mainly found in the F2 fraction at high Sm
385 concentrations, indicating that Sm was bound to carbonate minerals since ASCO has a very
386 low content of OM (LOI = 1.6%) and a high content of carbonates (38%). This behaviour
387 agrees with the published data demonstrating extremely high affinity of trivalent lanthanides
388 and actinides for certain carbonate minerals, such as aragonite, which occur less frequently in
389 soil than other carbonate-like minerals like calcite or dolomite (Sutton, 2009; Zhong et al.,
390 1995). Given that ASCO has the lowest clay content among the soils tested (except for the
391 peat soil DUBLIN), the presence of different types of carbonates in ASCO appears to be
392 responsible for its Sm sorption behaviour.

393 **4. Conclusions**

394 For some types of soils, the Sm sorption is highly dependent on the Sm concentration present
395 in solution. Whereas Sm sorption is high and strongly irreversible at low Sm concentrations,
396 at high Sm concentrations, only those soils with a large pool of high-affinity sorption sites for
397 Sm, i.e., slightly acidic peat soils (high content of slightly soluble organic matter) or alkaline
398 soils rich in clay and organic matter, present a linear Sm sorption capacity. For other types of
399 soil, it is expected a concentration-dependent capacity to sorb Sm, resulting in low Sm
400 retention at high Sm concentrations. Therefore, risk assessment models aiming at evaluating
401 the environmental impact of Sm contamination episodes should use the Sm sorption data that
402 better suits to the scenario under study by selecting them on Sm concentration basis. The
403 $K_{d,linear}$ values and sorption models developed in the present work can be used to estimate the

Sm interaction in soils presenting soil characteristics similar to those tested here, especially for screening purposes, in a wide range of contamination scenarios. Furthermore, it was demonstrated that K_d data gathered for low concentrations of stable Sm can be successfully applied to assess the interaction of Sm radioisotopes in soils affected by radioactive contamination events, which entails a remarkably advantage since K_d data for stable Sm is frequently much more available, or can be obtained more easily, than those for Sm radioisotopes.

Acknowledgements

This study was supported by the Ministerio de Ciencia e Innovación de España (CTM2014-55191) and the Generalitat de Catalunya (AGAUR 2014SGR1277). Oriol Ramírez was supported by an APIF pre-doctoral fellowship from the University of Barcelona.

References

Ali, H.A., 2014. Social and environmental impact of the rare earth industries. Resources 3, 123-134.

Awual, M.R., Kobayashi, T., Miyazaki, Y., Motokawa, R., Shiwaku, H., Suzuki, S., Okamoto, Y., Yaita, T., 2013. Selective lanthanide sorption and mechanism using novel hemodified adsorbent. J. Hazard. Mater. 252-253, 313-320.

Burt, R., 2004. Soil survey laboratory methods manual. Investigation report No 42, Version 4.0, Natural Resources Conservation Service, USDA, Washington, USA.

Cao, X., Wang, X., Zhao, G., 2000.Assessment of the bioavailability of rare earth elements in soils by chemical fractionation and multiple regression analysis. Chemosphere 40, 23-28.

Cao, X., Chen, Y., Wang, X., Deng, X., 2001. Effect of redox potential and pH value on the release of rare earth elements from soil. Chemosphere 44, 655-661.

427 Dupré, B., Viers, J., Dandurand, J.L., Polve, M., Bénézeth, P., Vervier, P., Braun, J.J., 1999.
428 Major and trace elements associated with colloids in organic-rich river waters:
429 ultrafiltration of natural and spiked solutions. Chem. Geol. 160, 63-80.

430 Fagerlund, G., 1973. Determination of specific surface by the BET method. Mater. Struct. 6
431 (3), 239-245.

432 Fan, Q.H., Zhang, M.L., Zhang, Y.Y., Ding, K.F., Yang, Z.Q., Wu, W.S., 2010. Sorption of
433 Eu(III) and Am(III) on attapulgite: effect of pH, ionic strength and fulvic acid.
434 Radiochim. Acta 98, 19-25.

435 Feng, L. X., Xiao, H. Q., He, X., Li, Z. J., Li, F. L., Liu, N. Q., 2005. Long-term effects of
436 lanthanum intake on the neurobehavioral development of the rat. Neurotoxicology and
437 Teratology, 28, 119–124.

438 Galunin. E., Alba, M.D., Avilés, M.A., Santos, M.J., Vidal, M., 2009. Reversibility of La and
439 Lu sorption onto smectites: implications for the design of engineered barriers in deep
440 geological repositories. J. Hazard. Mater. 172, 1198-1205.

441 Galunin. E., Alba, M.D., Santos, M.J., Abrão, T., Vidal, M., 2010. Lanthanide sorption on
442 smectitic clays in presence of cement lechates. Geochim. Cosmochim. Ac. 74, 862-875.

443 Geckeis, H., Rabung, T., 2008. Actinide geochemistry: From the molecular level to the real
444 system. J. Contam. Hydrol. 102, 187-195.

445 GRS, 2012. Radionuclide inventory of vitrified waste after spent nuclear fuel reprocessing at
446 La Hague. Gesellschaft für Anlagen- und Reaktorsicherheit, GRS-294, Germany.

447 He, J., Lü, C.W., Xue, H.X., Liang, Y., Bai, S., Sun, Y., Shen, L.L., Mi, N., Fan, Q.Y., 2010.
448 Species and distribution of rare earth elements in the Baotou section of the Yellow River
449 in China. Environ. Geochem. Healthmuller 32, 45-58.

450 Hinz, C., 2001. Description of sorption data with isotherm equations. Geoderma 99, 225–243.

451 Hirano, S., Suzuki, K. T., 1996. Exposure, metabolism, and toxicity of rare earths and related
452 compounds. Environmental Health Perspectives 104, 85–95.

453 Ho Lee, M., Chang, E., Song, K., Hee, Y., Sang, H., 2011. The influence of humic acid on the
454 pH-dependent sorption of americium (III) onto kaolinite. J. Radioanal. Nucl. Ch. 287, 639-
455 645.

456 Houba, V. J. G., Temminghoff, E. J. M., Gaishorst, G. A., van Wark, W., 2000. Soil analysis
457 procedures using 0.01 M calcium chloride as extraction reagent. Soil Sci. Plant Anal. 31,
458 1299-1396.

459 Humsa, T.Z., Srivastava, R.K., 2015. Impact of rare earth mining and processing on soils and
460 water environment at Chavara, Kollam, Kerala: a case study. Proc. Earth Planet. Sci. 11,
461 566 – 581.

462 Jin, Q., Wang, G., Ge, M., Chen, Z., Wu, W., Guo, Z., 2014. The adsorption of Eu (III) and
463 Am (III) on Beishan granite: XPS, EPMA, batch and modelling study. Appl. Geochem. 47,
464 17-24.

465 Jinxia, L., Mei, H., Xiuqin, Y., Jiliang, L., 2010. Effects of the accumulation of the rare earth
466 elements on soil macrofauna community. J. Rare Earth 28 (6), 957-964.

467 Jones, D.L., 1997. Trivalent metal (Cr, Y, Rh, La, Pr, Gd) sorption in two acid soils and its
468 consequences for bioremediation. Eur. J. Soil Sci. 48, 697-702.

469 Li, D., Huang, S., Wang, D., Wang, W., Peng, A., 2000. Transfer characteristics of rare earth
470 elements applied in agricultural soils. J.Environ. Sci. Health A 35 (10), 1869-1881.

471 Li, D., Huang, S., Wang, W., Peng, A., 2001. Study on the kinetics of cerium(III) adsorption-
472 desorption on different soils of China. Chemosphere 44, 663-669.

473 Li, X., Chen, Z., Chen, Z., Zhang, Y., 2013. A human health risk assessment of rare earth
474 elements in soil and vegetables from a mining area in Fujian Province, Southeast China.
475 Chemosphere 93, 1240-1246.
476 Liang, T., Zhang, S., Wang, L.J., Kung, H-T., Wang, Y.Q., Hu, A.T., Ding, S.M., 2005.
477 Environmental biogeochemical behaviors of rare earth elements in soil-plant systems.
478 Environ. Geochem. Health, 27, 301.
479 Liang, T., Li, K., Wang, L., 2014. State of rare earth elements in different environmental
480 components in mining areas of China. Environ. Monit. Assess. 186, 1499-1513.
481 Lu, G.C., Gao, Z. H., Meng, Y. X., Chen, Q., Ren, S. Y., Tang, X. K., 1995. Hygienic
482 investigation of different rare earth (RE) mining areas in China: RE levels of farmer's
483 natural living environment and head air. Chinese Journal of Environmental Science 4, 78-
484 82.
485 McCarthy, J.F., Sanford, W.E., Stafford, P.L., 1998. Lanthanide field tracers demonstrate
486 enhanced transport of transuranic radionuclides by natural organic matter. Environ. Sci.
487 Technol. 32, 3901-3906.
488 Meng, X.L., Ji, H.B., 2008. Advance in study on rare earth elements in waters and their
489 geochemistry. Journal of Capital Normal University (Natural Science Edition), 29, 64-68.
490 Moikin, G.Y., 1993. The establishment of the hygienic standard for the samarium content of
491 water. Gig. Sanit. Jan. 1, 24-5.
492 Mueller, G., Gastner, M., 1971. The "Karbonate-bomber", a simple device for the
493 determination of the carbonate content in sediments, soils, and other materials. Neues Jb.
494 Miner. Monat. 10, 466-469.
495 Pang, X., Li, D., Peng, A., 2001. Application of rare-earth elements in the agriculture of
496 China and its environmental behavior in soil. J. Soils Sediments 1(2), 124-129.

497 Pathak, P.N., Choppin, G.R., 2007. Sorption of Am^{3+} cations on suspended silicate: effects of
498 pH, ionic strength, complexing anions, humic acids and metal ions. J. Radioanal. Nucl.
499 Ch., 274 (3), 517-523.

500 Pourret, O., Martinez, R.E., 2009. Modeling lanthanide series binding sites on humic acid. J.
501 Colloid Interf. Sci. 330, 45-50.

502 Quevauviller, P., Rauret, G., Ure, A., Bacon, J., Muntau, H., 1997. The certification of the
503 EDTA and acetic acid-extractable contents (mass fractions) of Cd, Cr, Cu, Pb and Zn in
504 sewage sludge amended soils CRMs 483 and 484. European Commision, BCR
505 information, Reference materials. Report EUR 17127 EN, Belgium.

506 Ramírez-Guinart, O., Vidal, M., Rigol, A., 2016. Univariate and multivariate analysis to
507 elucidate soil properties governing americium sorption in soils. Geoderma 269, 19-26.

508 Ramírez-Guinart, O., Rigol, A., Vidal, M., 2017. Assessing soil properties governing
509 radiosamarium sorption in soils: can trivalent lanthanides and actinides be considered as
510 analogues**?** Geoderma 290, 33-39.

511 Rego, M.E., Vicente, R., Hiromoto, G., 2011. Temporal evolution of activities in wastes from
512 Mo-99 production. In: Proceedings of International Nuclear Atlantic Conference – INAC
513 (ISBN: 978-85-99141-04-5).

514 Shan, X.Q., Lian, J., Wen, B., 2002. Effect of organic acids on adsorption and desorption of
515 rare earth elements. Chemosphere 47, 701-710.

516 Shanbhag, P.M., Morse, J.W., 1981. Americium interaction with calcite and aragonite
517 surfaces in seawater. Geocim. Cosmochim. Ac. 46, 241-246.

518 Shand, C.A., Cheshire, M.V., Smith, S., Vidal, M., Rauret, G., 1994. Distribution of
519 radiocaesium in organic soils. J. Environ. Radioact. 23, 285-302.

520 Sutton, M., 2009. LLNL-SR-415700 Review of distribution coefficients for radionuclides in
521 carbonate materials, Lawrence Livermore National Laboratory, USA.

522 Takahashi, Y., Minai, Y., Kimura, T., Tominaga, T., 1998. Adsorption of europium (III) on
523 kaolinite and montmorillonite in the presence of humic acid. J. Radioanal. Nucl. Ch. 237,
524 277-282.

525 Tyler, G., 2004. Rare earth elements in soil and plant systems-A review. Plant Soil 267, 191-
526 206.

527 Wang, Z., Yu, X., Zhao, Z., 1989. The geochemistry of rare earth elements (p. 321). Science
528 Press, Beijing, China.

529 Wang, L., Liang, T., Chong, Z., Zhang, C., 2011. Effects of soil type on leaching and runoff
530 transport of rare earth elements and phosphorous in laboratory experiments. Environ. Sci.
531 Pollut. Res. 18, 38-45.

532 Wei, F., Zheng, C., Chen, J., Wu, Y., 1991.Study on the background contents on 61 elements
533 of soils in China. Chinese Journal of Environmental Science 12, 12-20.

534 Wenming, D., Xiangke, W., Xiaoyan, B., Aixia, W., Jingzhou, D., Zuyi, T., 2001.
535 Comparative study on sorption/desorption of radioeuropium on alumina, bentonite and red
536 earth: effects of pH, ionic strength, fulvic acid, and iron oxides in red earth. Appl. Radiat.
537 Isot. 54, 603-610.

538 Xiangke, W., Wenming, D., Xiongxin, D., Aixia, W., Jinzhou, D., Zuyi, T., 2000. Sorption
539 and desorption of Eu and Yb on alumina: mechanisms and effect of fulvic acid. Appl.
540 Radiat. Isot. 52, 165-173.

541 Ye, Y., Chen, Z., Montavon, G., Jin, Q., Guo, Z., Wu, W., 2014. Surface complexation
542 modeling of Eu(III) adsorption on silica in the presence of fulvic acid. Sci. China. Chem.
543 57 (9), 1276-1282.

544 Zhang, S., Shan, X.Q., Li, F., 2000. Low-molecular-weight organic-acids as extractant to
545 predict plant bioavailability of rare earth elements. Int. J. Environ. An. Ch. 76 (4), 283-
546 294.

547 Zhao, Y., Yu, R., Hu, G., Lin, X., Liu, X., 2017. Characteristics and environmental
548 significance of rare earth elements in $PM_{2.5}$ of Nanchang, China. J. Rare Earth 35 (1), 98-
549 106.

550 Zhong, S., Mucci, A., 1995. Partitioning of rare earth elements (REEs) between calcite and
551 seawater solutions at 25ºC and 1atm, and high dissolved REE concentrations. Geochim.
552 Cosmochim. Ac. 59, 443-453.

553 Zhu, J. G., Xing, G. X., Yamasaki, S., & Tsumura, A., 1993. Adsorption and desorption of
554 exogenous rare earth elements in soils: I. Rate of forms of rare earth elements sorbed.
555 Pedosphere 3, 299–308.

556 Zhu, W.F., Xu, S.Q., Shao, P.P., Zhang, H., Feng, J., Wu, D.L., Yang, W.J., 1997.
557 Investigation on intake allowance of rare earth – a study on bio-effect of rare earth in
558 South Jiangxi. Chin. Environ. Sci. 1, 63–65.

559 Zhu, J. H., Yuan, Z. K., Wang, X. Y., Yan, S. M., 2002. Investigation on the contents of rare
560 earth elements in environment of rare earth ore area in Jiangxi. Environmental Health, 19,
561 443–448.

562

563 **Table 1.** Summary of soil characteristics.

Soil sample	Solid phase							Liquid phase[a]						
	Clay (%wt)	Silt (%wt)	Sand (%wt)	$CaCO_3$ (%wt)	LOI (%wt)	CEC ($cmol_c\ kg^{-1}$)	SSA ($m^2\ g^{-1}$)	pH	DIC (mg L^{-1})	DOC (mg L^{-1})	Ca (mmol L^{-1})	Mg (mmol L^{-1})	K (mmol L^{-1})	Na (mmol L^{-1})
DELTA2	33.5	31.3	12.2	51	23	87.3	6.5	8.0	32	39	2.0	0.70	0.13	4.0
DUBLIN	1.3[b]	na	na	2	78	140	0.6	5.7	29	290	1.4	0.37	0.15	0.19
ANDCOR	18.3	23.6	39.1	2	19	54.2	4.5	4.9	1	78	0.10	0.37	0.08	0.13
CABRIL	20.0	16.5	57.5	2	6.0	19.3	9.5	6.4	3	10	0.12	0.12	0.05	0.05
ASCO	16.9	63.0	18.5	38	1.6	40.8	11.0	8.4	5	5	3.4	0.16	0.13	0.03

564 LOI, loss on ignition; CEC, cation exchange capacity; SSA, specific surface area; DIC, dissolved inorganic carbon; DOC, dissolved organic carbon.
565 Clay, silt and sand percentages are referred to the whole soil.
566 na: not analysed.
567 [a] Liquid phase refers to the supernatant obtained from sorption blank assays (see section 2.2).
568 [b] Clay content was obtained by X-ray diffraction.

569 **Table 2.** Sorption and desorption parameters of Sm in the tested soil samples.

Soil sample	Sorption				Desorption				$K_{d,des}/K_d$ ratio
	C_i (meq L^{-1})	C_{eq} (meq L^{-1})	K_d (L kg^{-1})	S (%)	$C_{i,des}$ (meq kg^{-1})	$C_{eq,des}$ (meq L^{-1})	$K_{d,des}$ (L kg^{-1})	D (%)	
DELTA2	0.01	1.8×10^{-5}	16,000	99.8	0.28	1.6×10^{-5}	18,000	0.1	1.1
	0.1	1.5×10^{-4}	16,000	99.8	2.5	1.3×10^{-4}	19,000	0.1	1.2
	2.9	4×10^{-3}	19,000	99.9	74	0.0042	18,000	0.1	1.0
	9.9	0.01	22,000	99.9	260	0.0098	27,000	0.1	1.2
DUBLIN	0.03	3.5×10^{-4}	2,200	98.7	0.75	1.7×10^{-4}	4,300	0.7	2.0
	0.3	3.5×10^{-3}	2,200	98.7	7.8	1.5×10^{-4}	5,400	0.5	2.4
	2.7	0.027	2,900	99.0	77	0.017	4,500	0.6	1.6
	9.4	0.068	3,400	99.4	233	0.051	5,300	0.5	1.6
ANDCOR	0.01	1.9×10^{-4}	1,400	98.2	0.28	1.1×10^{-4}	2,600	0.8	1.8
	0.1	1.7×10^{-3}	1,400	98.2	2.5	8.8×10^{-4}	2,800	0.7	1.9
	2.9	0.16	400	94.3	71	0.018	3,800	0.5	8.8
	9.8	4.9	26	50.2	128	0.097	1,300	1.6	50
CABRIL	0.03	1.3×10^{-4}	5,400	99.5	0.71	8×10^{-5}	8,900	0.3	1.6
	0.3	1.1×10^{-3}	6,700	99.6	7.3	9×10^{-4}	8,100	0.3	1.2
	3.1	0.013	6,000	99.6	78	0.0034	23,000	0.1	3.8
	9.6	4.5	29	53.4	132	0.071	1,800	1.4	62
ASCO	0.05	4.1×10^{-6}	300,000	>99.9	1.2	< lq	-	-	-
	0.2	1.4×10^{-4}	41,000	99.9	6.0	9.3×10^{-5}	64,000	0.04	1.6
	2.7	0.19	340	93.0	63	0.0019	21,000	0.1	63
	10.3	5.6	21	45.6	119	0.019	6,200	0.4	300

570 **Table 3.** Sorption parameters (confidence range, $p = 0.05$) derived from fitting Sm sorption isotherms to Freundlich, Langmuir and linear

571 equations. $K_{d,linear}$ (L kg^{-1}); K (L meq^{-1}); b (meq kg^{-1}); K_f ($meq^{(1-N)}$ L^N kg^{-1}) and N (dimensionless).

Soil sample	Sorption models
DELTA2	$K_{d,linear}$[a] = 17,000 (80) ; R^2 = 0.99
	Freundlich: K_f = 37,000 (15,000), N = 1.1 (0.1); R^2 = 0.99
DUBLIN	$K_{d,linear}$[a] = 2,400 (40); R^2 = 0.99
	Freundlich: K_f = 6,000 (1,000), N = 1.2 (0.1); R^2 = 0.99
ANDCOR	$K_{d,linear}$[a] = 1,400 (20); R^2 = 0.99
	Langmuir: K = 10 (4), b = 124 (13); R^2 = 0.99
CABRIL	$K_{d,linear}$[a] = 5,900 (100) ; R^2 = 0.99
	Langmuir: K = 90 (17), b = 132 (5); R^2 = 0.99
ASCO	$K_{d,linear}$[a] = 260,000 (75,000) ; R^2 = 0.92
	Freundlich: K_f = 81 (15), N = 0.23 (0.05); R^2 = 0.99

[a] Linear model at $C_i < 0.1$ meq L^{-1} for ASCO and at $C_i < 0.2$ meq L^{-1} for ANDCOR, CABRIL, DELTA2 and DUBLIN.

572

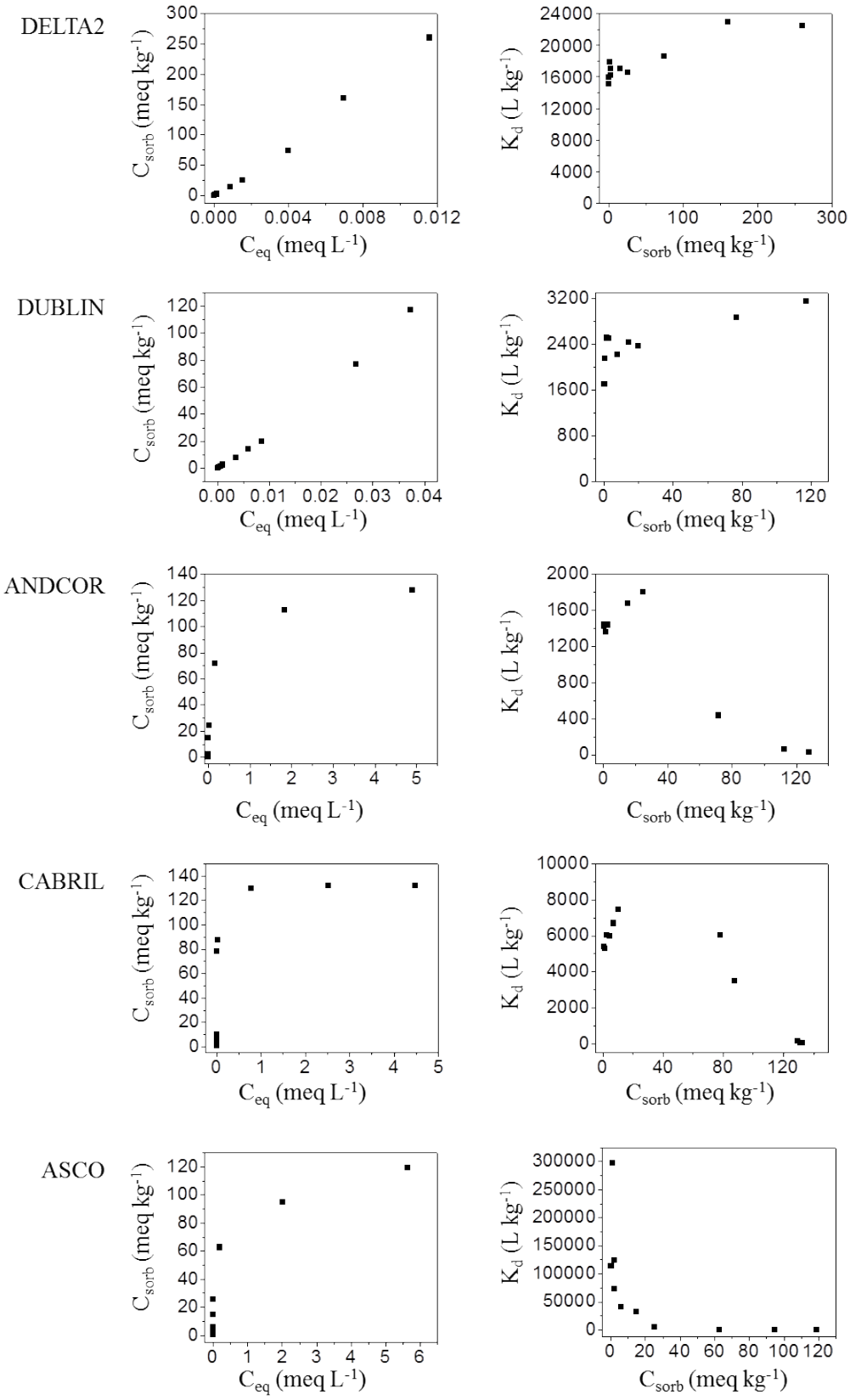

573

574 **Figure 1.** Sorption isotherms of Sm in the soil samples: C_{sorb} *vs.* C_{eq} and K_d *vs.* C_{sorb} plots.

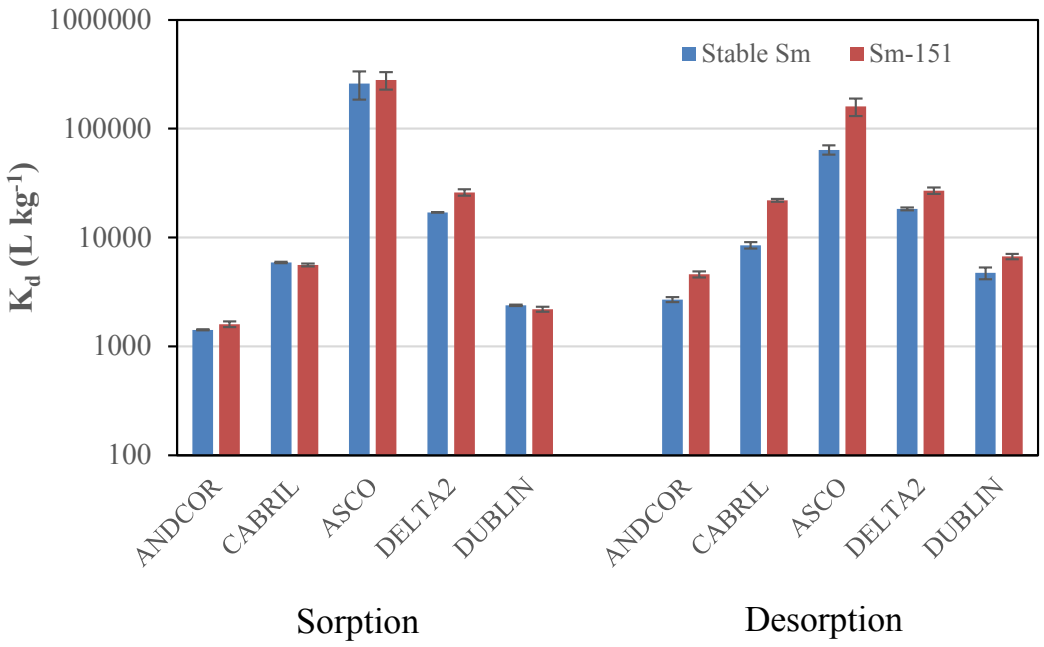

575

576 **Figure 2.** Comparison of the K_d values of stable Sm at low initial concentrations (C_i = 0.01 –

577 0.2 meq L^{-1}) and ^{151}Sm ($C_i = 10^{-5}$ meq L^{-1}). Error bars for the K_d values correspond to the

578 standard deviation of replicates (n= 3) for ^{151}Sm and to the confidence range of $K_{d,linear}$ for

579 stable Sm (p = 0.05).

580

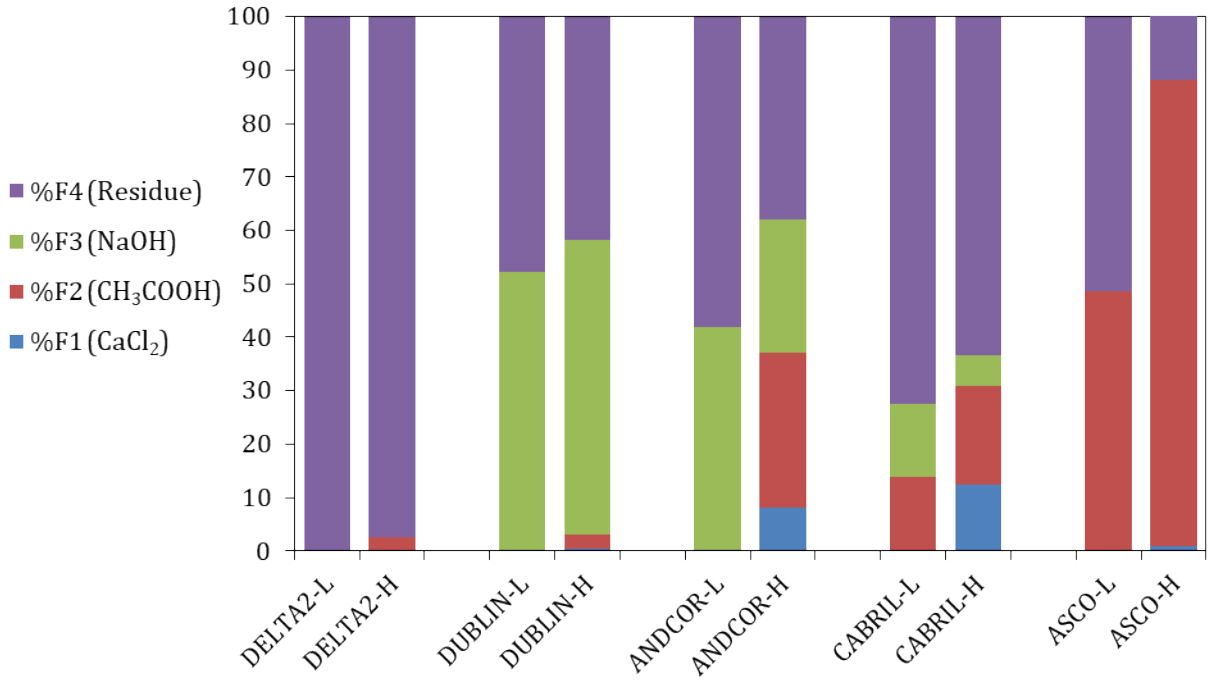

	DELTA2-L	DELTA2-H	DUBLIN-L	DUBLIN-H	ANDCOR-L	ANDCOR-H	CABRIL-L	CABRIL-H	ASCO-L	ASCO-H
C_{sorb} (meq kg^{-1})	1.49	160	1.52	117	1.45	113	1.05	130	2.35	94.7
S (%)	99.9	99.9	98.8	99.1	98.1	70.2	99.5	86.8	> 99.9	64.4
K_d (L kg^{-1})	18000	23000	2500	3100	1350	61	5300	170	125000	47

Figure 3. Fractionation of Sm sorbed into the soil residues obtained from sorption tests with a low (-L) and high (-H) initial Sm concentration.

Supplementary information

Dependence of samarium-soil interaction on samarium concentration: implications for environmental risk assessment

Oriol Ramírez-Guinart, Aitor Salaberria, Miquel Vidal and Anna Rigol

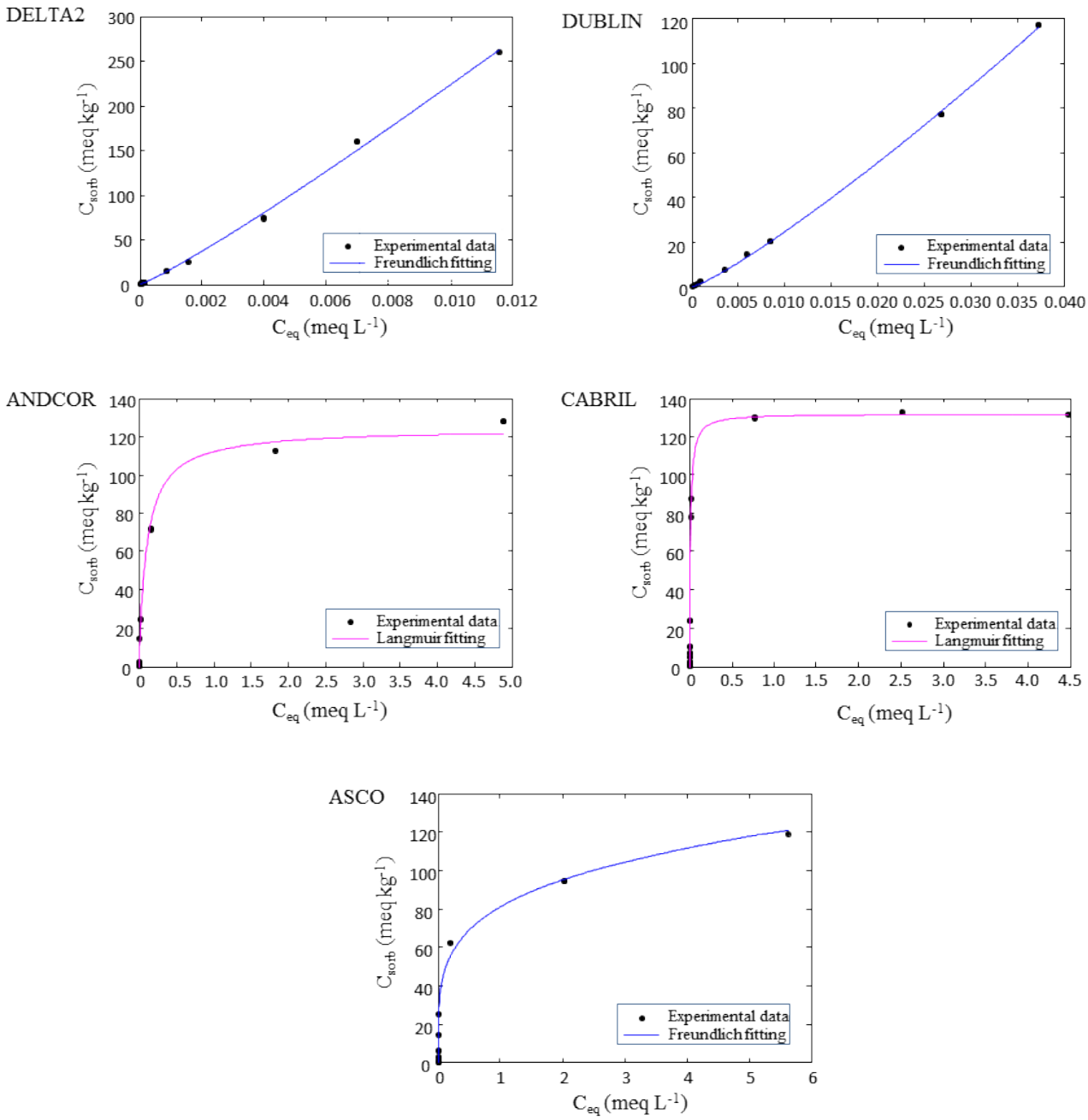

Figure S1. Graphical representation of the best fitting of the sorption isotherms for the whole range of concentrations.